THE JOURNAL OF BIOLOGICAL CHEMISTRY VOL. 289, NO. 32, pp. 22151–22160, August 8, 2014

Ras Promotes Transforming Growth Factor-β (TGF-β)-induced Epithelial-Mesenchymal Transition via a Leukotriene B_4 Receptor-2-linked Cascade in Mammary Epithelial Cells*

Received for publication, February 6, 2014, and in revised form, June 26, 2014 Published, JBC Papers in Press, July 2, 2014, DOI 10.1074/jbc.M114.556126

Hyunju Kim, Jung-A Choi, and Jae-Hong Kim[1]

From the College of Life Sciences and Biotechnology, Korea University, Seoul 136-701, Korea

Background: The mechanism by which oncogenic Ras contributes to epithelial-mesenchymal transition (EMT) is not clearly defined.
Results: The "BLT2-ROS-NF-κB"-linked cascade lies downstream of Ras and promotes EMT.
Conclusion: Activation of leukotriene B_4 receptor-2 (BLT2)-linked pathway contributes to EMT in mammary epithelial cells.
Significance: These findings suggest that BLT2 is a novel regulator of EMT in mammary epithelial cells.

Inflammation and inflammatory mediators are inextricably linked with epithelial-mesenchymal transition (EMT) through complex pathways in the tumor microenvironment. However, the mechanism by which inflammatory mediators, such as the lipid inflammatory mediators, eicosanoids, contribute to EMT is largely unknown. In the present study we observed that BLT2, leukotriene B_4 receptor-2, is markedly up-regulated by oncogenic Ras and promotes EMT in response to transforming growth factor-β (TGF-β) in mammary epithelial cells. Blockade of BLT2 by the BLT2 inhibitor LY255283 or by siRNA reduced EMT induced by Ras in the presence of TGF-β. In addition, stimulation of BLT2 by the addition of a BLT2 ligand, such as leukotriene B_4, restored EMT in the presence of TGF-β in human immortalized mammary epithelial MCF-10A cells. We further searched BLT2 downstream components and identified reactive oxygen species and nuclear factor κB as critical components that contribute to EMT. Taken together, these results demonstrate for the first time that a BLT2-linked inflammatory pathway contributes to EMT. This provides valuable insight into the mechanism of EMT in mammary epithelial cells. In addition, considering the implications of EMT with the stemness of cancer cells, our finding may contribute to a better understanding of tumor progression.

Epithelial-mesenchymal transition (EMT)[2] is a process essential for morphogenesis during embryonic development that has recently also been implicated in tumor metastasis (1). Through EMT, an epithelial cell alters its phenotype to that of a mesenchymal cell in response to stress or specific growth factors. This process is characterized by down-regulation of epithelial marker proteins, such as E-cadherin and zonula occludens-1 (ZO-1), and up-regulation of mesenchymal marker proteins, such as vimentin, N-cadherin, and fibronectin (1). It is currently thought that a subset of cancerous cells undergoes EMT to enable them to escape from surrounding cells, penetrate into neighboring lymph or blood vessels, and passage to distant sites to form secondary metastases (2, 3).

Transforming growth factor-β (TGF-β) is one of the key growth factors involved in driving EMT. Increased expression of TGF-β is observed in breast cancers, where it is associated with advanced stage, increased recurrence, and poor prognosis (4). Depending on the cellular context, TGF-β can induce EMT in cooperation with oncogenic Ras (5–7). Elevated expression of the oncogenic Ras protein has been found in 60–70% of human primary breast carcinomas, and thus Ras expression has been suggested as a marker of tumor aggressiveness in breast cancer (8). By synergistically promoting EMT in the presence of TGF-β, oncogenic Ras has been shown to collaborate with TGF-β to promote cell migration *in vitro* and tumor invasion and metastasis *in vivo* (5, 9). The mechanism by which oncogenic Ras contributes to EMT is not yet understood. Previously, we have shown that BLT2 lies downstream of Ras and mediates oncogenic Ras-induced transformation and invasion (10–12). The levels of leukotriene B_4 (LTB_4), one of the local lipid mediators in the inflammatory microenvironment, and its receptor, BLT2, are markedly up-regulated by oncogenic Ras and mediate Ras-associated tumorigenic activities (10–12). Expression of BLT2 in ovarian and breast cancer tissue is increased in advanced stages and is associated with poor clinical outcome (13–15). Furthermore, autocrine or paracrine BLT2 signaling mediates the invasiveness and metastasis of ovarian, bladder, and breast cancer cells (14, 16, 17).

Despite these observations implicating BLT2 as a potential mediator for aggressive metastatic cancer, its mechanism of action in EMT is not characterized. In the present study we found that BLT2 lies downstream of Ras and collaborates with TGF-β to induce EMT in mammary epithelial cells. We further examined BLT2 downstream components and identified reac-

* This work was supported by Bio and Medical Technology Development Program Grant 2012M3A9C5048709, Basic Science Research Program Grant 2012R1A2A2A01044526 through the National Research Foundation funded by the Ministry of Science, Information, and Communication Technologies (ICT) and Future Planning, Republic of Korea, and the National Research and Development Program for Cancer Control Grant 1220020, Ministry for Health and Welfare, Republic of Korea.
[1] To whom correspondence should be addressed: College of Life Sciences and Biotechnology, Korea University, 5-1 Anam-dong, Sungbuk-gu, Seoul, 136-701, Korea. Tel.: 82-2-3290-3452; Fax: 82-2-3290-3452; E-mail: jhongkim@korea.ac.kr.
[2] The abbreviations used are: EMT, epithelial-mesenchymal transition; LTB_4, leukotriene B_4; ROS, reactive oxygen species; Nox, NADPH oxidase.

tive oxygen species (ROS) and NF-κB as critical components that contribute to EMT.

EXPERIMENTAL PROCEDURES

Chemicals and Plasmid—U75302 and LY255283 were obtained from Biomol (Plymouth Meeting, PA). Bovine serum albumin (BSA), dimethyl sulfoxide (DMSO), cholera enterotoxin, hydrocortisone, epidermal growth factor (EGF), insulin, and 4′-6-diamidino-2-phenylindole (DAPI) were obtained from Sigma. Horse serum and Dulbecco's modified Eagle's medium/F-12 (DMEM/F-12) were obtained from Invitrogen. All other chemicals were from standard sources and were of molecular biology grade or higher. The human BLT2 (GenBank™ accession number NM_019839.1) plasmid was cloned by polymerase chain reactions (PCR) methods using a human genomic bacterial artificial chromosome (BAC) library as described previously (18, 19).

Cell Culture—Human immortalized mammary epithelial MCF-10A cells and Ha-Ras-overexpressing MCF-10A cells (MCF-10A/Hras) were a kind gift from Dr Moon Aree (Duksung Women's University, Seoul, South Korea) and were maintained in DMEM/F-12 medium containing 5% heat-inactivated horse serum, 10 μg/ml bovine insulin, 20 ng/ml EGF, 100 ng/ml cholera enterotoxin, 0.5 μg/ml hydrocortisone, 100 units/ml penicillin, and 100 unit/ml streptomycin. EpH4 and EpRas mouse mammary epithelial cells were kindly provided by Dr. Byung-Chul Kim (Kangwon National University, Chuncheon, South Korea) and were maintained in DMEM with 10% FBS. All cells were incubated at 37 °C in 5% CO_2.

Semiquantitative Reverse Transcription (RT)-PCR and Real-time Quantitative PCR Analysis—Total RNA was extracted from cells with Easy-Blue (Intron, Sungnam, Korea) and subjected to RT by incubation at 37 °C for 50 min in 20 μl of solution containing 0.5 μg of oligo$(dT)_{15}$ primer, 10 mM dithiothreitol, 0.5 mM deoxynucleoside triphosphates, and 200 units of Moloney murine leukemia virus reverse transcriptase (Beams Biotechnology, Kyunggi, Korea) followed by PCR amplification of each transcript with the use of a RT-PCR PreMix kit (Intron). The primer sequences used are as follows (forward and reverse, respectively): BLT1 (5′-TATGTCTGCGGAGTCAGCATGTACGC-3′ and 5′-CCTGTAGCCGACGCCCTATGTCCG-3′) (20); BLT2 (5′-AGCCTGGAGACTCTGACCGCTTTCG-3′ and 5′-GACGTAGCACCGGGTTGACGCTA-3′) (20); E-cadherin (5′-TGGAGGAATTCTTGCTTTGC-3′ and 5′-CGTACATGTCAGCCAGCTTC-3′) (21); vimentin (5′-GACACTATTGGCCGCCTGCAGGATGAG-3′ and 5′-CTGCAGAAAGGCACTTGAAAGC-3′), (22); Nox4 (5′-CTCAGCGGAATCAATCAGCTGTG-3′ and 5′-AGAGGAACACGACAATCAGCCTTAG-3′) (20); snail (5′-GCTCCTTCGTCCTTCTCCTC-3′ and 5′-TGACATCTGAGTGGGTCTGG-3′) (23); and glyceraldehyde-3-phosphate dehydrogenase (GAPDH) (5′-CTGCACCACCAACTGCTTAGC-3′ and 5′-CTTCACCACCTTCTTGATGTC-3′ (20). The detailed protocol for PCR involved 30 cycles (BLT1, BLT2, and Nox4), 20 cycles (GAPDH), or 23 cycles (E-cadherin, vimentin, and snail) of denaturation at 95 °C for 30 s, annealing at 67 °C (BLT1, BLT2), 58 °C (E-cadherin, vimentin, and GAPDH), 62 °C (Nox4), or 60 °C (snail) for 20 s, and elongation at 72 °C for 40 s. The sizes of the amplification products are 346 bp (BLT1), 321 bp (BLT2), 380 bp (E-cadherin), 413 bp (vimentin), 418 bp (Nox4), 286 bp (snail), and 376 bp (GAPDH). Nox1 mRNA was analyzed using two-step RT-PCR as described previously (24). For the first-round PCR, the primers 5′-CAGGGAGACAGGTGCCTTTTCC-3′ (forward) and 5′-GCTCAAACCTGACGAGACCAAG-3′ (reverse) were used, and for the second round, nested PCR with the primers 5′-AACCTGTTGACTTCCCTGGAAC-3′ (forward) and 5′-TCCAGACTGGAATATCGGTGAC-3′ (reverse) (designed from GenBank™ accession number 007052) was performed. The amplification protocol for both the first round and nested PCR included 27 cycles of denaturation 95 °C for 30 s, annealing at 61 °C for 40 s, and elongation at 72 °C for 45 s. For Nox1, the size of amplification product is 305 bp. The primers for mouse BLT1 were 5′-GCATGTCCCTGTCTCGTT-3′ (forward) and 5′-CGGGCAAAGGCCTTAGTACG-3′ (reverse), and the primers for mouse BLT2 were 5′-CAGCATGTACGCCAGCGTGC-3′ (forward) and 5′-CGATGGCGCTCACCAGACG-3′ (reverse) (25). The PCR protocol for mouse BLT1/2 entailed 35 cycles of denaturation at 94 °C for 30 s, annealing at 68 °C for 30 s, and elongation at 72 °C for 30 s followed by extension at 72 °C for 10 min. The sizes of the amplification products for mouse BLT1 and BLT2 are 364 and 380 bp, respectively. The specificity of all primers was confirmed by sequencing the PCR products. All PCR products were resolved by 1.5% agarose gel electrophoresis visualized by staining with ethidium bromide and photographed with a GelDoc system (Bio-Rad). For quantification, gels were scanned, and the pixel intensity for each band was determined using the ImageJ program (NIH Image, Bethesda, MD) and normalized to the amount of GAPDH.

For real-time quantitative PCR analysis, total RNA extracted from cells using the easy-BLUE RNA extraction kit (Intron) was subjected to RT with Moloney murine leukemia virus reverse transcriptase (Beams Biotechnology). The BLT1, BLT2, and GAPDH cDNAs were amplified as described previously (15) with SYBR Green I-based real-time PCR using a LightCycler 480 instrument (Roche Applied Science). The quantification data were analyzed with LightCycler software 3.3 (Roche Diagnostics). The melting curves were analyzed to ensure the specificity of amplification. Primers (forward and reverse, respectively) for real-time PCR analysis were 5′-CCTGAAAAGGATGCAGAAGC-3′ and 5′-AAAAAGGGAGCAGTGAGCAA-3′ for human BLT1 and 5′-CTTCTCATCGGGCATCACAG-3′ and 5′-ATCCTTCTGGGCCTACAGGT-3′ for human BLT2.

Three-dimensional Collagen Assay—Depending on the final volume required, calculated amounts of 10 × phosphate-buffered saline (PBS), 5 N sodium hydroxide (NaOH), and type I rat tail collagen (BD Biosciences; final concentration 2 mg/ml) were prepared. The pH was adjusted to 7.4 ± 0.05, and the solutions were kept on ice for up to 30 min before use. Wells of a 24-well dish were pre-coated with 200 μl of collagen solution. Cells were harvested, washed 3 times with PBS, and resuspended at 3×10^4 cells/ml in the collagen solution. A 300-μl volume of cell suspension was laid over the bottom layer. After gelling, complete culture medium was added and changed every 2–3 days. Morphology was assessed on day 9 by image capture at ×20 magnifications.

Invasion Assay—To monitor the invasion potential of MCF-10A and MCF-10A/Hras cells, BD BioCoat™ Matrigel™ Invasion Chambers (BD Biosciences) were used. Cells (5×10^4) were removed from culture plates with trypsin-EDTA, washed in DMEM/F-12 containing 0.5% serum, and seeded on top of the rehydrated Matrigel inserts. As a chemoattractant, DMEM/F-12 containing 5% serum was added to the lower chamber, and plates were incubated at 37 °C for 48 h. The membranes were fixed in methanol and stained with hematoxylin and eosin (H&E) stain. The contents of the upper membrane surface were then removed, and invasive cells were microscopically counted in four random high power fields per filter; each sample was assayed in triplicate, and the assays were performed three times.

Flow Cytometric Analysis of BLT2—For quantitation of BLT2 expression, cells were incubated in 60-mm dishes for 24 h. The cells were detached by treatment with trypsin, washed with PBS, and fixed in 2% paraformaldehyde and then permeabilized with 0.1% Triton X-100 for 10 min. After exposure to 2% BSA for 30 min, they were incubated for 1 h at room temperature with rabbit polyclonal antibodies to BLT2 (1:100 dilution; Cayman Chemical, Ann Arbor, MI), washed 3 times with PBS, and incubated for 30 min at room temperature with fluorescein isothiocyanate-conjugated goat antibodies to rabbit immunoglobulin G (1:200 dilution; Molecular Probes, Eugene, OR). The cells (10,000 per sample) were then subjected to flow cytometry using a FACSCalibur instrument and Cell Quest software (BD Biosciences) for determination of mean fluorescence intensity.

RNA Interference—Scrambled and BLT2-specific siRNA (5′-CCACGCAGUCAACCUUCUG-3′) were purchased from Bioneer (Daejeon, Korea) (26). The mammalian expression vectors pSUPER-siNox1 and pSUPER-siNox4 were provided by Dr. Yoon-Soo Bae (Ewha Women's University, Seoul, Korea). The Nox1/4 target sequences were previously described (27). The siRNAs and siRNA vector were introduced into cells as instructed in Opti-MEM (Invitrogen) using Oligofectamine or Lipofectamine reagents (Invitrogen), respectively. After 24 h, the mRNA levels of each gene were analyzed by RT-PCR to evaluate interference.

Immunofluorescence Staining of E-cadherin and Vimentin—Cells were cultured as a monolayer on glass coverslips (24 × 24 mm), washed twice with PBS, fixed with 4% paraformaldehyde in PBS for 10 min, permeabilized with 0.1% Triton X-100 for 10 min, and washed 3 times in PBS. They were blocked with 2% BSA in PBS for 30 min at room temperature and incubated for 60 min with primary antibodies (1:100 dilution for E-cadherin, 1:100 dilution for vimentin; Santa Cruz Biotechnology, Santa Cruz, CA) and then with fluorescein isothiocyanate- or tetramethylrhodamine isothiocyanate-conjugated secondary antibodies (1:200 dilution; Molecular Probes) for 45 min. Each step was performed in PBS containing 2% BSA, and the cells were washed 3 times for 5 min with the same solution between steps. The integrity of the nuclei was confirmed by DAPI (Sigma) staining. The coverslips were mounted on 25 × 75-mm microslides using 90% glycerol, examined with a confocal laser-scanning microscope (510META; Carl Zeiss, Oberkochen, Germany).

Western Blotting—Adherent cells were collected and lysed with buffer (40 mM Tris·HCl, pH 8.0, 120 mM NaCl, 0.1% Nonidet-P40, 100 mM phenylmethylsulfonyl fluoride, 1 mM sodium orthovanadate, 2 μg/ml leupeptin, 2 μg/ml aprotinin). Proteins were separated by sodium dodecyl sulfate polyacrylamide gel electrophoresis and transferred to a nitrocellulose membrane. The membrane was blocked with 5% nonfat dry milk in Tris-buffered saline and incubated with primary antibodies against E-cadherin, vimentin, p-IκB-α, IκB-α,and α-tubulin for 1 h at room temperature. Blots were developed with a peroxidase-conjugated secondary antibody, and proteins were visualized by enhanced chemiluminescence (Amersham Biosciences).

Measurement of ROS—Intracellular hydrogen peroxide (H_2O_2) was measured in cells plated in 60-mm dishes. Actively growing cells were incubated for 10 min in the dark at 37 °C with 20 μM 2′,7′-dichlorofluorescein diacetate, after which dichlorofluorescein fluorescence was measured by flow cytometry with a FACSCalibur (BD Biosciences).

Luciferase Reporter Assay for NF-κB Activity—MCF-10A and MCF-10A/Hras cells were transfected with 1.4 μg of NF-κB luciferase reporter gene (28) using Lipofectamine reagent (Invitrogen). To monitor variations in cell numbers and transfection efficiency, MCF-10A and MCF-10A/Hras cells were co-transfected with 0.6 μg pSV40-β-galactosidase, a eukaryotic expression vector containing the *Escherichia coli* β-galactosidase (*lacZ*) structural gene under the control of the SV40 promoter. After 24 h in complete medium, starvation with 0.5% horse serum for 3 h, and treatment with TGF-β for 48 h, the cells were harvested and assayed for luciferase activity as described (28).

Data Analysis and Statistics—The data are representative of three independent experiments. Results are presented as the means ± S.D. Analyses were performed with Student's *t* test using SigmaPlot 8.0 software. *p* values less than 0.05 were considered significant.

RESULTS

Ras Collaborates with TGF-β to Potentiate EMT in Mammary Epithelial Cells—It has been shown that Ras collaborates with TGF-β to induce EMT in several epithelial cell models (5–7, 29). In the present study we used MCF-10A immortalized human mammary epithelial cells, which have a round cobblestone-like morphology (Fig. 1*A*). In addition, we used MCF-10A/Hras cells expressing oncogenic H-Ras, which exhibit a partial morphological alteration from round cobblestone-like to fibroblast-like cells. Treatment of MCF-10A/Hras cells with TGF-β further generated a fibroblast-like elongated shape and induced a loss of cell-cell contact, which is typical of EMT (Fig. 1*A*), concomitant with a decrease in the expression of E-cadherin and an increase in that of vimentin, as examined by semiquantitative RT-PCR and immunoblot analysis (Fig. 1*B*). The same sets of cells were evaluated for morphology in three-dimensional culture. Cells that have undergone EMT are known to exhibit a branched morphology in three-dimensional matrix. As shown in Fig. 1*C*, after treatment with TGF-β, MCF-10A/Hras cells exhibited highly branched structures, typical of EMT. EMT was also shown to cause increased motility and invasiveness, thus promoting tumor metastasis (30). We, therefore, determined invasiveness using a modified Boyden chamber assay. MCF-10A/Hras cells stimulated with TGF-β were

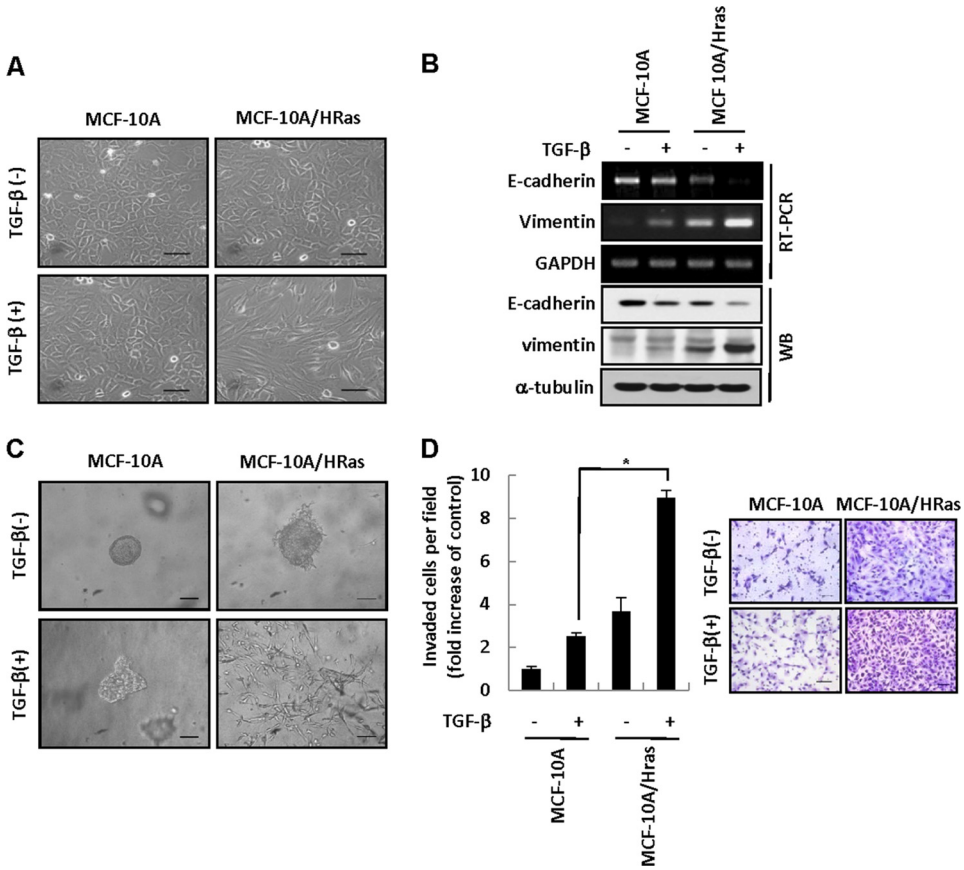

FIGURE 1. **Ras promotes EMT in response to TGF-β in mammary epithelial cells.** *A*, human immortalized mammary epithelial MCF-10A cells and MCF-10A/Hras cells were incubated with TGF-β (5 ng/ml) for 48 h and visualized using an Olympus BX51 microscope at $\times$20 magnification. *Scale bars*, 100 μm. *WB*, Western blot. *B*, cells treated as in *A* were subjected to semiquantitative RT-PCR analysis or immunoblot analysis for E-cadherin and vimentin. *C*, MCF-10A and MCF-10A/Hras cells were propagated in three-dimensional cultures for 9 days in the absence or presence of TGF-β (5 ng/ml), at which point alterations in morphology were visualized using an Olympus BX51 microscope at $\times$20 magnification. *Scale bars*, 100 μm. *D*, MCF-10A and MCF-10A/Hras cells were assayed for invasiveness in the presence of TGF-β (5 ng/ml) for 48 h. Representative invading cells stained with H&E are shown, and quantitative data are shown as the mean $\pm$ S.D. of three independent experiments. *Scale bars*, 100 μm. *, $p < 0.05$.

more invasive than TGF-β-stimulated MCF-10A cells (Fig. 1*D*). Together, these results suggest that Ras promotes EMT in response to TGF-β in MCF-10A cells.

Blockade of BLT2 Significantly Reduced EMT Promoted by Ras—To elucidate the downstream components of Ras signaling in EMT induced in MCF-10A/Hras cells in response to TGF-β, we first analyzed BLT2 expression. In agreement with a previous report (10), expression of BLT2, but not BLT1, was elevated by Ras, as detected by semiquantitative RT-PCR and quantitative real-time PCR analysis (Fig. 2*A*). Consistent with these results, the abundance of BLT2 protein as determined by flow cytometry was higher in MCF-10A/Hras cells than in MCF-10A cells (Fig. 2*B*). In contrast, TGF-β treatment did not affect transcript levels of BLT2 (Fig. 2*C*). We next examined whether BLT2 plays any role in EMT triggered by Ras. Treatment of MCF-10A/Hras cells with BLT2 inhibitor LY255283 or depletion of BLT2 with a BLT2-specific small interfering RNA (siBLT2) greatly reduced the morphological alterations (Fig. 2, *D* and *H*) and the changes in epithelial and mesenchymal marker expression (Fig. 2, *E* and *I*). In contrast, the BLT1 inhibitor U75302 had no effect on morphology and epithelial/mesenchymal marker expression (Fig. 2, *D* and *E*). Similarly, in three-dimensional culture, development of the branched morphology of MCF-10A/Hras cells in response to TGF-β was dramatically inhibited by LY255283 or siBLT2 knockdown (Fig. 2, *F* and *J*). Next, we examined whether BLT2 contributed to the increased invasion observed in MCF-10A/Hras cells in response to TGF-β. Application of LY255283 or siBLT2 knockdown reduced the invasiveness of MCF-10A/Hras cells in response to TGF-β (Fig. 2, *G* and *K*). Together, these results suggest that BLT2 lies downstream of Ras and contributes to EMT.

BLT2 Cooperates with TGF-β to Induce EMT in Mammary Epithelial Cells—To further examine the contribution of BLT2 in signaling the EMT in mammary epithelial cells, we examined whether BLT2 could collaborate with TGF-β to drive EMT in MCF-10A cells. For this test, MCF-10A cells were treated with LTB_4, an agonist of BLT2. Treating MCF-10A cells with LTB_4 alone had no significant effect on either morphology (Fig. 3*A*) or EMT marker expression (Fig. 3, *B* and *C*). In addition, TGF-β treatment alone partially decreased expression of E-cadherin and partly increased expression of vimentin (Fig. 3, *B* and *C*). However, co-treatment of the cells with LTB_4 and TGF-β markedly promoted the change in morphology, with cells adapting a spindle-like fibroblastic shape (Fig. 3*A*) and EMT marker expression (Fig. 3, *B* and *C*). To confirm the collaboration between BLT2 and TGF-β, we transiently transfected MCF-10A cells with BLT2 expression plasmid. The addition of

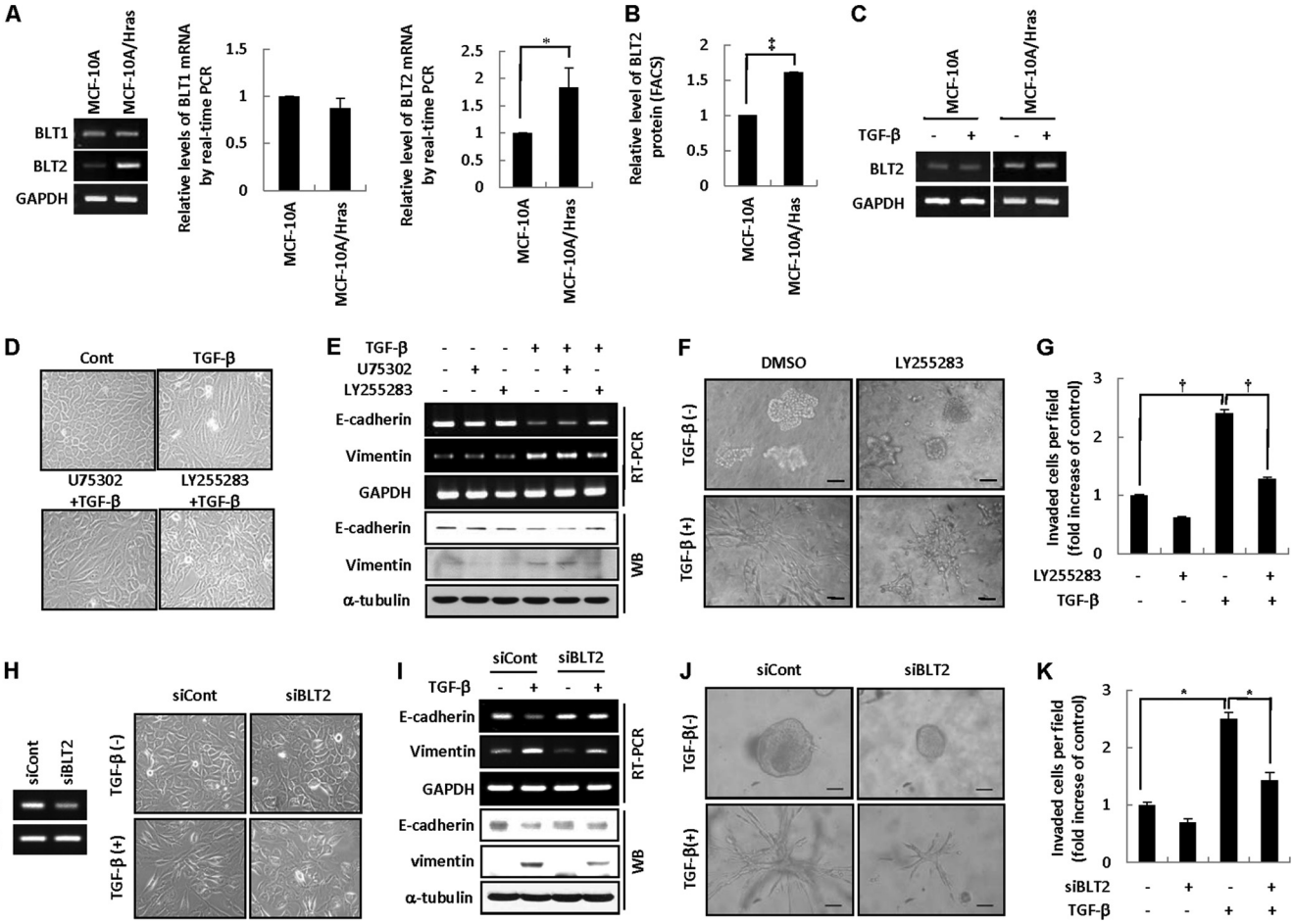

FIGURE 2. **Blockade of BLT2 significantly abrogated EMT promoted by Ras.** *A*, semiquantitative RT-PCR (*left panels*) and quantitative real-time PCR (*center* and *right panels*) analysis of BLT1 and BLT2 mRNAs in human immortalized mammary epithelial MCF-10A cells (control) as well as MCF-10A/Hras cells. *B*, flow cytometric analysis of BLT2 expression. *C*, MCF-10A and MCF-10A/Hras cells were incubated with TGF-β (5 ng/ml) for 48 h before determination of the abundance of BLT2 mRNAs by semiquantitative RT-PCR analysis. *D*, MCF-10A/Hras cells pretreated with U75302 (0.5 μM) and LY255283 (2.5 μM) for 30 min were simulated with TGF-β (5 ng/ml) for 48 h and then visualized using an Olympus BX51 microscope at $\times$ 20 magnification. *E*, cells treated as in *D* were subjected to semiquantitative RT-PCR analysis or immunoblot analysis for E-cadherin and vimentin. *F*, MCF-10A/Hras cells were propagated in three-dimensional cultures for 9 days in the absence or presence of LY255283 (2.5 μM) or TGF-β (5 ng/ml), at which point alterations in morphology were visualized using an Olympus BX51 microscope at $\times$20 magnification. *Scale bar*, 100 μm. *G*, MCF-10A/Hras cells were incubated with LY255283 (2.5 μM) or DMSO vehicle for 30 min and then assayed for invasiveness in the continued presence of LY255283 (2.5 μM) and TGF-β (5 ng/ml) for 48 h. *H*, MCF-10A/Hras cells were transfected with BLT2 (*siBLT2*) or control (*siCont*) siRNAs for 48 h, after which the amounts of BLT2 mRNAs were determined by semiquantitative RT-PCR (*left panels*). MCF-10A/Hras cells were transfected with BLT2 or control siRNAs for 24 h before TGF-β (5 ng/ml) treatment for 48 h. The cells were visualized using an Olympus BX51 microscope at $\times$20 magnification (*right panels*). *I*, MCF-10A/Hras cells were treated as in *H* (*right panels*), after which the expressions of E-cadherin and vimentin were determined by semiquantitative RT-PCR analysis or immunoblot analysis. *J*, MCF-10A/Hras cells were transfected with BLT2 or control siRNAs for 24 h. The cells were then propagated in three-dimensional cultures for 9 days in the absence or presence of TGF-β (5 ng/ml), at which point alterations in morphology were visualized using an Olympus BX51 microscope at $\times$20 magnification. *Scale bars*, 100 μm. *K*, MCF-10A/Hras cells were transfected with BLT2 or control siRNAs for 24 h and then assayed for invasiveness in the presence of TGF-β (5 ng/ml) for 48 h. All quantitative data are shown as the mean $\pm$ S.D. of three independent experiments. *, $p < 0.05$; †, $p < 0.01$; ‡, $p < 0.005$.

TGF-β to these BLT2-transfected cells markedly reduced levels of E-cadherin and enhanced levels of vimentin (Fig. 3*D*). Also, in three-dimensional collagen culture, TGF-β induced branching in BLT2-overexpressing MCF-10A cells (Fig. 3*E*). Moreover, overexpression of BLT2 in MCF-10A cells markedly enhanced TGF-β-induced invasiveness (Fig. 3*F*). Together, these results suggest that BLT2 and TGF-β can collaborate to induce EMT in mammary epithelial cells.

"Nox1-ROS" Lied Downstream of BLT2 and Contributed to EMT—ROS play important roles in EMT and the mobility of many cell types (31). Also, our previous observations suggested that ROS production lies downstream of BLT2 in Ras signaling leading to transformation or during cancer progression (11, 12, 16). We, therefore, examined whether ROS functions downstream of BLT2 to promote EMT in MCF-10A/Hras cells. First, the ROS levels in MCF-10A and MCF-10A/Hras cells were examined. With the use of the redox-sensitive fluorescent probe dichlorofluorescein, we found that intracellular ROS production was increased in MCF-10A/Hras cells compared with MCF-10A cells (Fig. 4*A*). However, this increase in ROS levels in MCF-10A/Hras cells was reduced by depletion of BLT2 by siRNA (Fig. 4*B*), suggesting that BLT2 mediates ROS production in MCF-10A/Hras cells.

We recently reported that BLT2 up-regulates NADPH oxidase (Nox) (12, 15, 17, 32). Therefore, we determined whether BLT2 plays a role in the Nox up-regulation in MCF-10A/Hras cells. Clearly, the level of Nox1 mRNA, but not that of Nox4 mRNA, in MCF-10A/Hras cells was reduced by LY255283 (Fig.

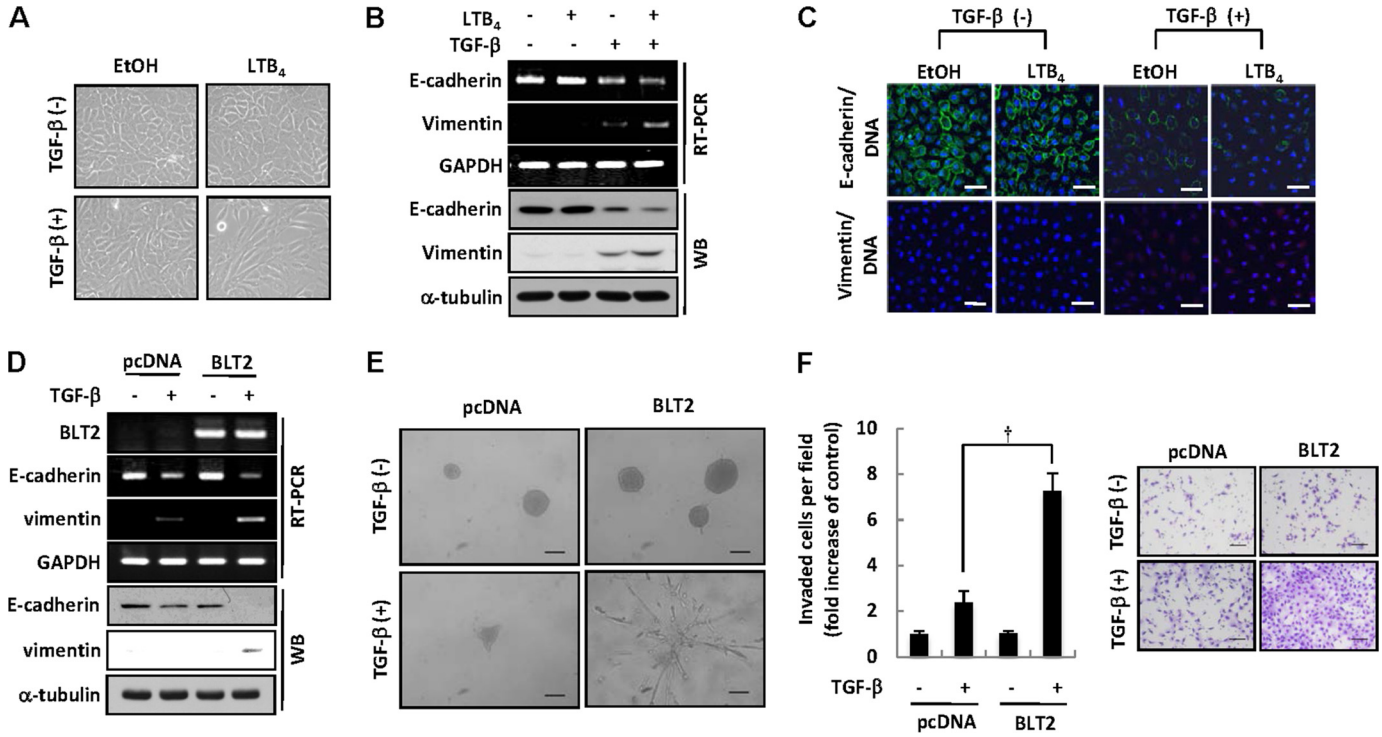

FIGURE 3. **BLT2 cooperates with TGF-β to induce EMT in mammary epithelial cells.** *A*, human immortalized mammary epithelial MCF-10A cells were pretreated with LTB_4 (300 nM) or ethanol (EtOH) for 30 min before TGF-β (5 ng/ml) treatment for 48 h. The cells were visualized using an Olympus BX51 microscope at × 20 magnification. *B*, MCF-10A cells treated as in *A* were subjected to semiquantitative RT-PCR analysis or immunoblot analysis of E-cadherin and vimentin. *C*, MCF-10A cells treated as in A were subjected to immunofluorescence staining for E-cadherin (*green*) and vimentin (*red*). DAPI (*blue*) was used to stain nuclei. The results shown are representative of three randomly photographed fields with similar results. Original magnification, × 400. *Scale bars*, 50 μm. *D*, MCF-10A cells were transfected with a vector for BLT2 or the corresponding empty vector for 24 h, after which the cells were treated with or without TGF-β (5 ng/ml) for 48 h for determination of the amount of E-cadherin and vimentin using semiquantitative RT-PCR or immunoblot analysis. *E*, MCF-10A cells transfected with a vector for BLT2 or the corresponding empty vector for 24 h were propagated in three-dimensional cultures for 9 days in the absence or presence of TGF-β (5 ng/ml), at which point alterations in morphology were visualized using an Olympus BX51 microscope at ×20 magnification. *Scale bar*, 100 μm. *F*, MCF-10A cells were transfected with a vector for BLT2 or the corresponding empty vector for 24 h and then assayed for invasiveness in the presence of TGF-β (5 ng/ml) for 48 h. Representative invading cells stained with H&E are shown, and quantitative data are shown as the mean ± S.D. of three independent experiments. *Scale bars*, 100 μm. †, $p < 0.01$.

4*C*, *left panels*) or by siBLT2 knockdown (Fig. 4*C*, *right panels*), whereas U75302 had no such effect (data not shown). Interestingly, TGF-β was found to induce Nox4 up-regulation (Fig. 4, *C* and *D*). Overexpression of BLT2 markedly enhanced Nox1 mRNA, but not Nox4 mRNA (Fig. 4*D*), suggesting that Nox1 functions downstream of BLT2. Consistent with these results, depletion of Nox1 by siRNA resulted in marked inhibition of ROS generation in MCF-10A/Hras cells (Fig. 4*E*). It also markedly attenuated the changes in epithelial and mesenchymal marker expression induced by TGF-β treatment (Fig. 4*F*). Together, these results suggest that "'Nox1-derived ROS production" lies downstream of BLT2 and promotes EMT in the presence of TGF-β.

NF-κB Lies Downstream of BLT2-ROS and Contributes to EMT—The transcription factor NF-κB has been identified as a central mediator of EMT in a mouse model of breast cancer progression (33). In addition, increased production of ROS has been shown to activate NF-κB (34). We, therefore, determined whether NF-κB contributes to EMT triggered by Ras in the presence of TGF-β. To do this, MCF-10A/Hras cells were pretreated with the NF-κB inhibitor Bay11-7082 before stimulation with TGF-β. As expected, this reduced the changes in E-cadherin and vimentin expression in MCF-10A/Hras cells in the presence of TGF-β (Fig. 5*A*). We next examined whether NF-κB lies downstream of the BLT2-ROS cascade in MCF-10A/Hras cells. Immunoblot analysis of p-IκB-α and IκB-α revealed that NF-κB activation was markedly enhanced in MCF-10A/Hras cells compared with in MCF-10A cells (Fig. 5*B*). And depletion of BLT2 by siRNA resulted in marked attenuation of the NF-κB activation (Fig. 5*C*). To further study the role of the BLT2-ROS cascade in the activation of NF-κB, MCF-10A cells were stimulated by increasing the concentration of LTB_4 alone or in combination with TGF-β, and NF-κB activation was measured by immunoblot analysis of p-IκB-α and IκB-α. As shown in Fig. 5*D*, the addition of LTB_4 enhanced the phosphorylation of IκB-α and degradation of IκB-α in response to TGF-β. Moreover, BLT2 overexpression enhanced the phosphorylation of IκB-α and degradation of IκB-α in response to TGF-β (Fig. 5*E*). We also determined the activity of an NF-κB luciferase reporter gene and found that BLT2 depletion by siBLT2 in MCF-10A/Hras cells inhibited NF-κB luciferase activity in response to TGF-β (Fig. 5*F*). In addition, BLT2 stimulation by either treatment with LTB_4 or overexpressing BLT2 markedly enhanced NF-κB luciferase activity in response to TGF-β (Fig. 5, *G* and *H*). Finally, we found that depletion of Nox1 with siRNA markedly inhibited the phosphorylation of IκB-α and degradation of IκB-α (Fig. 5*I*). Together, these results suggest that NF-κB activation lies downstream of the

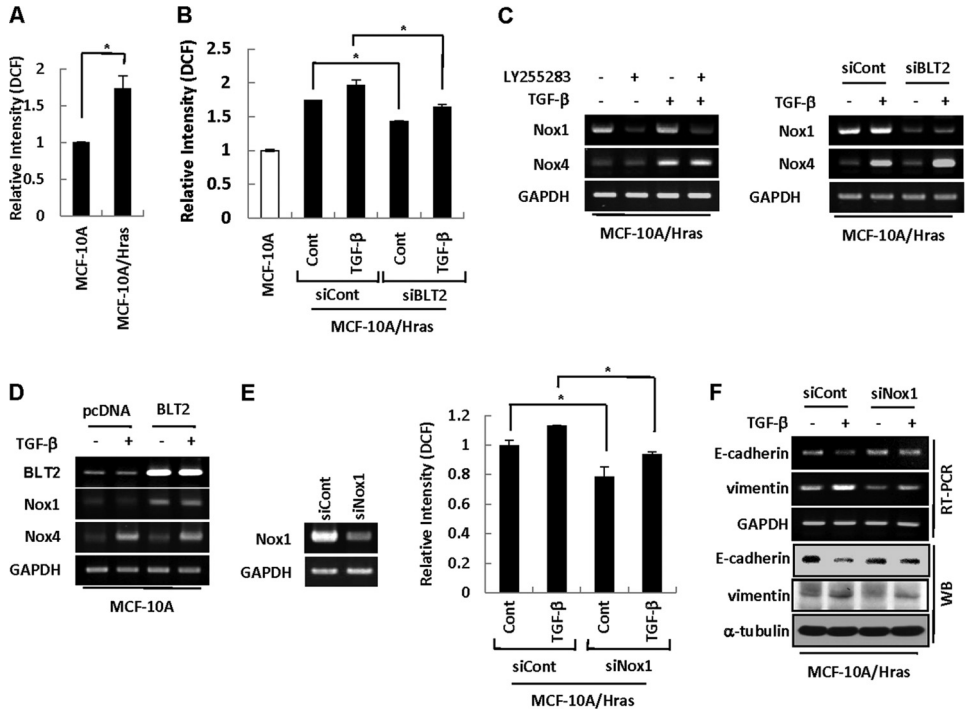

FIGURE 4. **Nox1-ROS lie downstream of BLT2 and contribute to EMT.** *A*, human immortalized mammary epithelial MCF-10A cells and MC-10A/Hras cells were incubated in the presence of 0.5% serum for 3 h and then loaded with the diacetate form of dichlorofluorescein (*DCF*) (20 μM) for 10 min. Intracellular ROS levels were then determined by flow cytometric analysis of dichlorofluorescein fluorescence. *B*, MCF-10A/Hras cells were transfected with BLT2 or control siRNAs for 24 h before TGF-β (5 ng/ml) treatment for 48 h and then monitored for ROS levels. *C*, MCF-10A/Hras cells were incubated with LY255283 (2.5 μM) or DMSO for 30 min or were transfected with BLT2 or control siRNAs for 24 h. The cells were then treated with or without TGF-β (5 ng/ml) for 48 h for determination of the abundance of Nox1 and Nox4 mRNAs by semiquantitative RT-PCR analysis. *D*, MCF-10A cells were transfected with a vector for BLT2 or the corresponding empty vector for 24 h. Then the cells were treated with or without TGF-β (5 ng/ml) for 48 h, after which the amounts of Nox1 and Nox4 mRNAs were determined by semiquantitative RT-PCR. *E*, MCF-10A/Hras cells were transfected with a vector for Nox1 siRNA (pSUPER-siNox1) or the corresponding empty vector for 48 h, after which the amounts of Nox1 mRNAs were determined by semiquantitative RT-PCR (*left panels*). The cells were transfected with a vector for Nox1 siRNA (pSUPER-siNox1) or the corresponding empty vector for 24 h and then treated with or without TGF-β (5 ng/ml) for 48 h. Then, the cells were analyzed for the intracellular level of ROS (*right panel*). All quantitative data are the mean $\pm$ S.D. of three independent experiments. *, $p < 0.05$. *F*, MCF-10A/Hras cells were transfected as in (*E*, *right panels*), after which the amount of E-cadherin and vimentin were assessed by semiquantitative RT-PCR and immunoblot analysis (*WB*).

BLT2-Nox1-ROS cascade in the signaling to EMT in mammary epithelial cells as summarized in Fig. 5*J*.

DISCUSSION

In this study we have shown that BLT2 lies downstream of Ras and contributes to EMT through collaboration with the TGF-β signaling pathway in human mammary epithelial cells. In addition, we analyzed the key components mediating the BLT2 signaling to EMT and found that the Nox1-ROS-NF-κB cascade appears to be downstream of BLT2. Our findings provide important insights into the mechanism of EMT in mammary epithelial cells.

Elevated amounts of the oncogenic Ras protein have been found in 60–70% of primary breast carcinomas, and thus Ras expression has been suggested to be a marker of tumor aggressiveness in breast cancer (6, 8). Previous reports have suggested that oncogenic Ras cooperates with TGF-β to induce EMT in both mammary and keratinocyte-derived tumors and to drive tumor metastasis (35). Despite these reports implicating Ras in EMT, the downstream pathway of Ras mediating EMT has not been previously characterized. The results of the present study clearly demonstrate that BLT2 up-regulation lies downstream of Ras and contributes to EMT through collaboration with the TGF-β signaling pathway in mammary epithelial cells (Fig. 2). In support of BLT2 as a mediator of EMT, treatment with LTB_4 or overexpression of BLT2 induced enhanced EMT in the presence of TGF-β (Fig. 3). These results suggest that BLT2 and TGF-β somehow collaborate to fully induce EMT in mammary epithelial cells. To further examine the contributing role of BLT2 in EMT in mammary epithelial cells, we tested another cell line, EpH4, mouse mammary epithelial cells. Previously, EpH4 cells were shown to undergo EMT by cooperation between TGF-β and Ras (6). Using EpH4 and EpRas cells (EpH4 cells expressing oncogenic Ras) (6), we obtained results that were quite similar to those in MCF-10A and MCF-10A/Hras cells. For example, the expression of BLT2 was elevated in EpRas cells compared with EpH4 control cells (Fig. 6*A*). Also, the depletion of BLT2 with siBLT2 significantly attenuated the TGF-β-induced changes in protein levels of E-cadherin and vimentin in EpRas cells (Fig. 6*B*), together again supporting the role of BLT2 in EMT in mammary epithelial cells.

We evaluated the signaling pathways involved in the stimulation of EMT by BLT2 in response to TGF-β. Previous studies have shown that TGF-β drives EMT predominantly via the Smad2/3 signaling pathway (36, 37). In this study we found that TGF-β-mediated phosphorylation of Smad2/3 was not affected by altering BLT2 (Fig. 6*C*), suggesting that the BLT2 cascade is independent of Smad2/3 phosphorylation. In a previous report TGF-β was shown to collaborate with activated mutants of Ras,

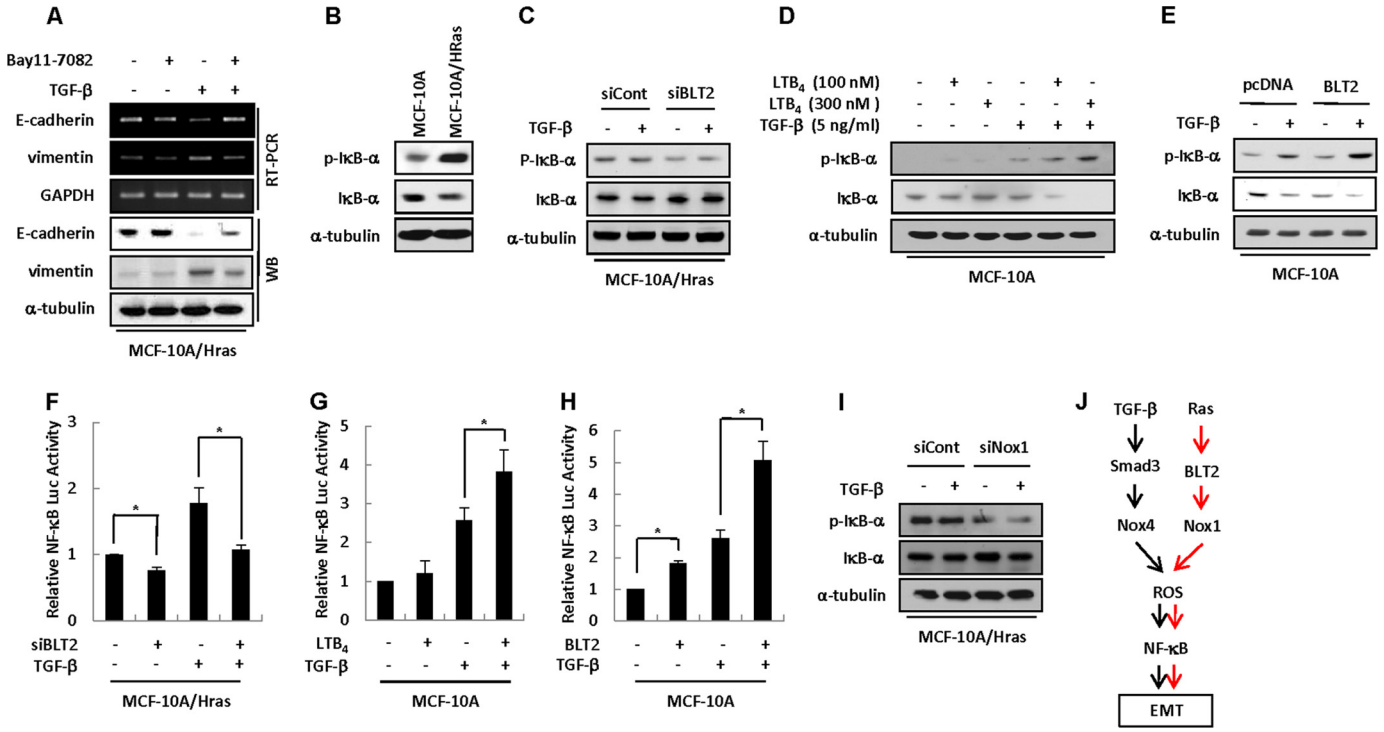

FIGURE 5. **NF-κB lies downstream of BLT2-ROS and contributes to EMT.** *A*, MCF-10A/Hras cells pretreated with Bay11-7082 (5 μM) for 30 min were simulated with TGF-β (5 ng/ml) for 48 h, and then the amounts of E-cadherin and vimentin were assessed by semiquantitative RT-PCR or immunoblot analysis (*WB*). *B–E*, MCF-10A and MCF-10A/Hras cells were incubated in the presence of 0.5% serum for 48 h (*B*). MCF-10A/Hras cells were transfected with BLT2 or control siRNAs for 24 h and then stimulated with TGF-β (5 ng/ml) for 48 h (*C*). MCF-10A cells were pretreated with LTB_4 (100 and 300 nM) or ethanol (EtOH) for 30 min before TGF-β (5 ng/ml) treatment for 48 h (*D*). MCF-10A cells were transfected with a vector for BLT2 or the corresponding empty vector for 24 h before TGF-β (5 ng/ml) treatment for 48 h (*E*). The cell lysates were subjected to immunoblot analysis for p-IκB-α and IκB-α. *F–H*, MCF-10A/Hras cells were transiently transfected with BLT2 or control siRNAs and the pNF-κB-Luc reporter plasmid for 24 h and then stimulated with TGF-β (5 ng/ml) for 48 h. The cells were harvested (*F*). Alternatively, MCF-10A cells were transiently transfected with pNF-κB-Luc reporter plasmid for 24 h. The cells were pretreated with LTB_4 (300 nM) or EtOH for 30 min, and then TGF-β (5 ng/ml) was added. After 48 h the cells were harvested (*G*). MCF-10A cells were transiently transfected with a vector for BLT2 or the corresponding empty vector and the pNF-κB-Luc reporter plasmid for 24 h and then stimulated with TGF-β (5 ng/ml) for 48 h. The cells were harvested (*H*). All cells were then assayed for relative luciferase activity. All quantitative data are the mean ± S.D. of three independent experiments. *, $p < 0.05$. *I*, MCF-10A/Hras cells were transfected with a vector for Nox1 siRNA (pSUPER-siNox1) or the corresponding empty vector for 24 h and then stimulated with TGF-β (5 ng/ml) for 48 h. The cell lysates were subjected to immunoblot analysis as in *B*. *J*, scheme for the involvement of BLT2-linked inflammatory pathway in EMT in mammary epithelial cells.

which activate constitutive extracellular signal-regulated kinases (ERK), to induce EMT in numerous epithelial cell types (6). In the MCF-10A system described here, we found that PD98059, an inhibitor of ERK, attenuated TGF-β-induced EMT. However, the BLT2 inhibitor LY255283 had no effect on the phospho-ERK levels of MCF-10A/Hras cells (data not shown), suggesting that the ERK pathway does not function downstream of BLT2 in EMT. We propose that NF-κB lies downstream of BLT2 and promotes TGF-β-induced EMT. We found that TGF-β-induced EMT was attenuated by the selective NF-κB inhibitor Bay11-7082 (Fig. 5*A*), and activation of NF-κB was suppressed by BLT2 knockdown (Fig. 5, *C* and *F*). In addition, previous studies have shown that the transcription factor NF-κB is a central mediator of EMT in a mouse model of breast cancer progression (33). In support of BLT2 as a mediator of NF-κB activation, overexpression of BLT2 induced enhanced NF-κB activation in the presence of TGF-β (Fig. 5, *E* and *H*). Furthermore, co-stimulation with TGF-β and LTB_4 increased NF-κB activation compared with either factor alone (Fig. 5, *D* and *G*). Therefore, these results suggest that synergistic regulation of NF-κB activation is an important component of the collaborative effect of oncogenic Ras and TGF-β signaling in mammary epithelial cells and that NF-κB activation in response to both TGF-β and BLT2 may be a key convergent point with a role in the inflammatory accentuation of EMT. Consistent with the role of NF-κB in EMT, activation of NF-κB has been shown to promote the transcription of the EMT regulators (*e.g.* snail and ZEB1/2). For example, it was reported that the activation of Snail transcription requires NF-κB; the Snail promoter has functional NF-κB sites (38), and the inhibition of NF-κB significantly reduced Snail transcription (39, 40). In addition, Chua *et al.* (41) reported that NF-κB suppresses the expression of E-cadherin and induces the expression of the mesenchyme-specific gene vimentin in MCF-10A cells through ZEB1/2. Consistent with those reports, we observed that inhibition of NF-κB with Bay11-7082 significantly diminished TGF-β-induced snail expression (Fig. 6*D*) and attenuated TGF-β-induced E-cadherin suppression (Fig. 5*A*) in MCF-10A/Hras cells. Because our results (Fig. 5, *C–H*) demonstrated that NF-κB activation lies downstream of BLT2 in the signaling to EMT, we next examined whether the inhibition or stimulation of BLT2 affects the expression of snail. BLT2 knockdown with siRNA clearly reduced snail expression in MCF-10A/Hras cells in the presence of TGF-β (Fig. 6*E*), and BLT2 transfection followed by LTB_4 treatment in MCF-10A cells further increased the expres-

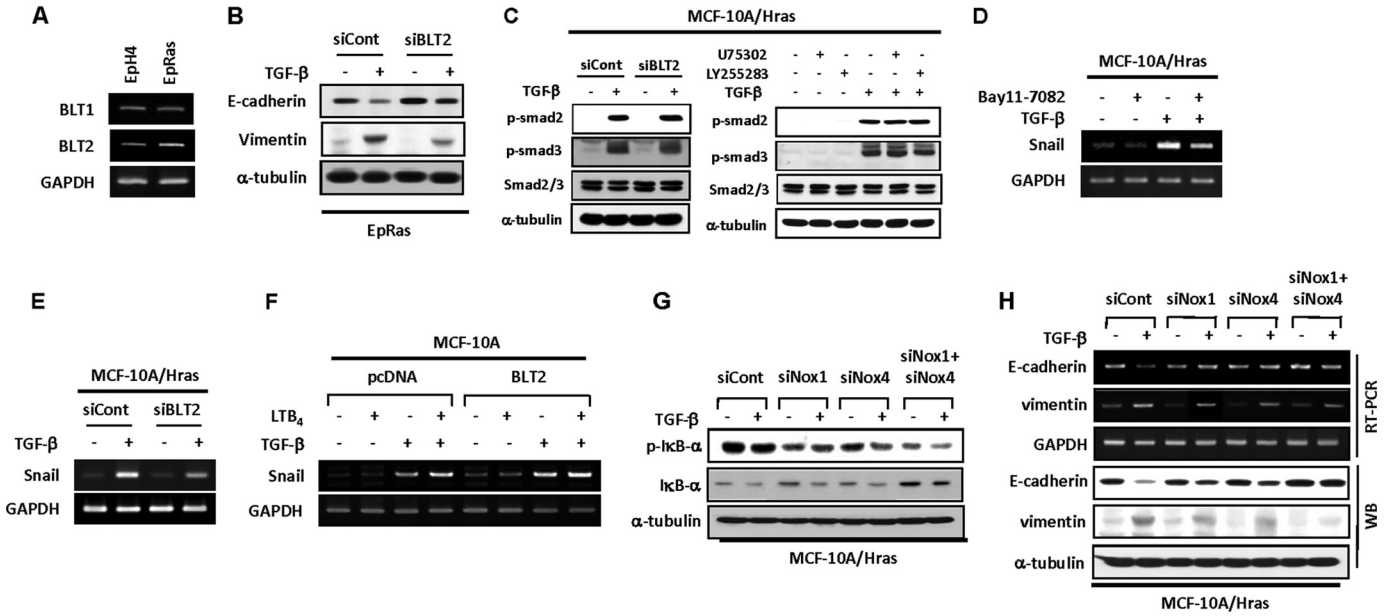

FIGURE 6. **BLT2 cascade is independent of Smad2/3 phosphorylation and Snail lies downstream of BLT2-NOX1-ROS-NF-κB.** *A*, semiquantitative RT-PCR analysis of BLT1 and BLT2 mRNAs in mouse mammary epithelial EpH4 cells (control) and EpRas cells. *B*, EpRas cells were transfected with BLT2 or control siRNAs for 24 h and then stimulated with TGF-β (5 ng/ml) for 48 h, after which the expressions of E-cadherin and vimentin were determined by immunoblot analysis. *C*, MCF-10A/Hras cells were transfected with BLT2 or control siRNAs for 24 h and then stimulated with TGF-β (5 ng/ml) for 48 h before immunoblot analysis for phospho-Smad2/3, Smad2/3, and α-tubulin (*left panels*). In addition, MCF-10A/Hras cells were pretreated with U75302 (0.5 μM) or LY255283 (2.5 μM) for 30 min before simulation with TGF-β (5 ng/ml) for 48 h, and then the cell lysates were subjected to immunoblot analysis for phospho-Smad2/3, Smad2/3 and α-tubulin (*right panels*). *D*, MCF-10A/Hras cells were pretreated with Bay11-7082 (5 μM) for 30 min before simulation with TGF-β (5 ng/ml) for 48 h, and then the amount of Snail was assessed by semiquantitative RT-PCR analysis. *E*, MCF-10A/Hras cells were transfected with BLT2 or control siRNAs for 24 h and then stimulated with TGF-β (5 ng/ml) for 48 h. Then the cells were subjected to semiquantitative RT-PCR analysis for Snail. *G*, MCF-10A cells were transfected with a vector for BLT2 or the corresponding empty vector for 24 h, after which the cells were pretreated with LTB_4 (300 nM) or ethanol (EtOH) for 30 min before TGF-β (5 ng/ml) treatment for 48 h. Then the cells were subject to semiquantitative RT-PCR analysis for Snail. *G*, MCF-10A/Hras cells were transfected with a vector for Nox1 siRNA (pSUPER-siNox1), Nox4 siRNA (pSUPER-siNox4), or the corresponding empty vector for 24 h and then treated with or without TGF-β (5 ng/ml) for 48 h. The cells were subjected to immunoblot analysis for p-IκB-α and IκB-α. *H*, cells were treated as in *H* and then the cell lysates were subjected to semiquantitative RT-PCR or immunoblot (*WB*) analysis for E-cadherin and vimentin.

sion of snail (Fig. 6*F*). These findings support a role of BLT2-NFκB in the activation of EMT regulators such as snail.

Our studies suggest that Nox1-derived ROS generation lies upstream of NF-κB activation in the BLT2-signaling cascade to EMT. We observed that Nox1 lies downstream of BLT2 and Nox1-induced ROS generation accentuates TGF-β-driven EMT via NF-κB activation. These results are consistent with previous reports suggesting that ROS are involved in EMT (42). We have shown that knockdown of Nox1 by siRNA attenuates ROS generation as well as TGF-β-induced EMT. Boudreau *et al.* (43) recently reported that Nox4 contributes to NADPH oxidase-dependent ROS production, which may be critical for the progression of EMT in breast epithelial cells. They demonstrated that phosphorylation of Smad3 positively regulates the human Nox4 promoter in breast epithelial cells. Similarly, we found that the level of Nox4 mRNA, but not that of Nox1 mRNA, was markedly increased by exposure to TGF-β (Fig. 4, *C* and *D*). However, we showed that the TGF-β-induced up-regulation of Nox4 mRNA was not inhibited by knockdown of BLT2 (Fig. 4*C*). It is possible that BLT2-induced Nox1 and TGF-β-induced Nox4 collaborate to fully induce EMT in mammary epithelial cells. For example, BLT2-Nox1-derived ROS and TGF-β-Nox4-derived ROS may additively stimulate NF-κB activation. In support of this idea, we found that depletion of both Nox1 and Nox4 by the appropriate siRNA led to a further dramatic inhibition of NF-κB activation (Fig. 6*G*) and changes in EMT markers (*e.g.* E-cadherin and vimentin) (Fig. 6*H*).

In any event, based on our observations, we propose a model that links the Ras and BLT2 signaling pathways and leads to accentuation of TGF-β-induced EMT in mammary epithelial cells. As summarized in Fig. 5*J*, our data reveal that up-regulation of BLT2 by oncogenic Ras results in the generation of ROS via Nox1 that together with NF-κB are probable downstream components of the BLT2-Nox1-ROS cascade, with potential roles in EMT associated with the collaboration of Ras with TGF-β. Identification of this novel mechanism may contribute to a better understanding of the mechanism of EMT.

REFERENCES

1. Thiery, J. P., and Sleeman, J. P. (2006) Complex networks orchestrate epithelial-mesenchymal transitions. *Nat. Rev. Mol. Cell Biol.* **7,** 131–142
2. Thiery, J. P. (2002) Epithelial-mesenchymal transitions in tumour progression. *Nat. Rev. Cancer* **2,** 442–454
3. Hugo, H., Ackland, M. L., Blick, T., Lawrence, M. G., Clements, J. A., Williams, E. D., and Thompson, E. W. (2007) Epithelial-mesenchymal and mesenchymal-epithelial transitions in carcinoma progression. *J. Cell Physiol.* **213,** 374–383
4. Teicher, B. A. (2001) Malignant cells, directors of the malignant process: role of transforming growth factor-β. *Cancer Metastasis Rev.* **20,** 133–143
5. Oft, M., Peli, J., Rudaz, C., Schwarz, H., Beug, H., and Reichmann, E. (1996) TGF-β1 and Ha-Ras collaborate in modulating the phenotypic plasticity and invasiveness of epithelial tumor cells. *Genes Dev.* **10,** 2462–2477
6. Janda, E., Lehmann, K., Killisch, I., Jechlinger, M., Herzig, M., Downward,

J., Beug, H., and Grünert, S. (2002) Ras and TGFβ cooperatively regulate epithelial cell plasticity and metastasis: dissection of Ras signaling pathways. *J. Cell Biol.* **156,** 299–313
7. Safina, A. F., Varga, A. E., Bianchi, A., Zheng, Q., Kunnev, D., Liang, P., and Bakin, A. V. (2009) Ras alters epithelial-mesenchymal transition in response to TGFβ by reducing actin fibers and cell-matrix adhesion. *Cell Cycle* **8,** 284–298
8. Clair, T., Miller, W. R., and Cho-Chung, Y. S. (1987) Prognostic significance of the expression of a ras protein with a molecular weight of 21,000 by human breast cancer. *Cancer Res.* **47,** 5290–5293
9. Lehmann, K., Janda, E., Pierreux, C. E., Rytömaa, M., Schulze, A., McMahon, M., Hill, C. S., Beug, H., and Downward, J. (2000) Raf induces TGFβ production while blocking its apoptotic but not invasive responses: a mechanism leading to increased malignancy in epithelial cells. *Genes Dev.* **14,** 2610–2622
10. Yoo, M. H., Song, H., Woo, C. H., Kim, H., and Kim, J. H. (2004) Role of the BLT2, a leukotriene B4 receptor, in Ras transformation. *Oncogene* **23,** 9259–9268
11. Kim, E. Y., Seo, J. M., Cho, K. J., and Kim, J. H. (2010) Ras-induced invasion and metastasis are regulated by a leukotriene B4 receptor BLT2-linked pathway. *Oncogene* **29,** 1167–1178
12. Choi, J. A., Kim, E. Y., Song, H., Kim, C., and Kim, J. H. (2008) Reactive oxygen species are generated through a BLT2-linked cascade in Ras-transformed cells. *Free Radic. Biol. Med.* **44,** 624–634
13. Rocconi, R. P., Kirby, T. O., Seitz, R. S., Beck, R., Straughn, J. M., Jr., Alvarez, R. D., and Huh, W. K. (2008) Lipoxygenase pathway receptor expression in ovarian cancer. *Reprod. Sci.* **15,** 321–326
14. Seo, J. M., Park, S., and Kim, J. H. (2012) Leukotriene B4 receptor-2 promotes invasiveness and metastasis of ovarian cancer cells through signal transducer and activator of transcription 3 (STAT3)-dependent up-regulation of matrix metalloproteinase 2. *J. Biol. Chem.* **287,** 13840–13849
15. Choi, J. A., Lee, J. W., Kim, H., Kim, E. Y., Seo, J. M., Ko, J., and Kim, J. H. (2010) Pro-survival of estrogen receptor-negative breast cancer cells is regulated by a BLT2-reactive oxygen species-linked signaling pathway. *Carcinogenesis* **31,** 543–551
16. Kim, E. Y., Seo, J. M., Kim, C., Lee, J. E., Lee, K. M., and Kim, J. H. (2010) BLT2 promotes the invasion and metastasis of aggressive bladder cancer cells through a reactive oxygen species-linked pathway. *Free Radic. Biol. Med.* **49,** 1072–1081
17. Kim, H., Choi, J. A., Park, G. S., and Kim, J. H. (2012) BLT2 up-regulates interleukin-8 production and promotes the invasiveness of breast cancer cells. *PLoS ONE* **7,** e49186
18. Haribabu, B., Zhelev, D. V., Pridgen, B. C., Richardson, R. M., Ali, H., and Snyderman, R. (1999) Chemoattractant receptors activate distinct pathways for chemotaxis and secretion. Role of G-protein usage. *J. Biol. Chem.* **274,** 37087–37092
19. Kim, J. Y., Lee, W. K., Yu, Y. G., and Kim, J. H. (2010) Blockade of LTB_4-induced chemotaxis by bioactive molecules interfering with the BLT2-$G\alpha_i$ interaction. *Biochem. Pharmacol.* **79,** 1506–1515
20. Seo, J. M., Cho, K. J., Kim, E. Y., Choi, M. H., Chung, B. C., and Kim, J. H. (2011) Up-regulation of BLT2 is critical for the survival of bladder cancer cells. *Exp. Mol. Med.* **43,** 129–137
21. Pan, Y., Lei, T., Teng, B., Liu, J., Zhang, J., An, Y., Xiao, Y., Han, J., Pan, X., Wang, J., Yu, H., Ren, H., and Li, X. (2011) Role of vimentin in the inhibitory effects of low molecular weight heparin on PC-3M cell adhesion to, and migration through, endothelium. *J. Pharmacol. Exp. Ther.* **339,** 82–92
22. Donaldson, A. E., Cai, J., Yang, M., and Iacovitti, L. (2009) Human amniotic fluid stem cells do not differentiate into dopamine neurons *in vitro* or after transplantation *in vivo*. *Stem Cells Dev.* **18,** 1003–1012
23. Kabashima-Niibe, A., Higuchi, H., Takaishi, H., Masugi, Y., Matsuzaki, Y., Mabuchi, Y., Funakoshi, S., Adachi, M., Hamamoto, Y., Kawachi, S., Aiura, K., Kitagawa, Y., Sakamoto, M., and Hibi, T. (2013) Mesenchymal stem cells regulate epithelial-mesenchymal transition and tumor progression of pancreatic cancer cells. *Cancer Sci.* **104,** 157–164
24. Chamulitrat, W., Schmidt, R., Tomakidi, P., Stremmel, W., Chunglok, W., Kawahara, T., and Rokutan, K. (2003) Association of gp91phox homolog Nox1 with anchorage-independent growth and MAP kinase-activation of transformed human keratinocytes. *Oncogene* **22,** 6045–6053
25. Cho, K. J., Seo, J. M., Lee, M. G., and Kim, J. H. (2010) BLT2 Is upregulated in allergen-stimulated mast cells and mediates the synthesis of Th2 cytokines. *J. Immunol.* **185,** 6329–6337
26. Hennig, R., Osman, T., Esposito, I., Giese, N., Rao, S. M., Ding, X. Z., Tong, W. G., Büchler, M. W., Yokomizo, T., Friess, H., and Adrian, T. E. (2008) BLT2 is expressed in PanINs, IPMNs, pancreatic cancer and stimulates tumour cell proliferation. *Br. J. Cancer* **99,** 1064–1073
27. Park, H. S., Lee, S. H., Park, D., Lee, J. S., Ryu, S. H., Lee, W. J., Rhee, S. G., and Bae, Y. S. (2004) Sequential activation of phosphatidylinositol 3-kinase, β Pix, Rac1, and Nox1 in growth factor-induced production of H_2O_2. *Mol. Cell. Biol.* **24,** 4384–4394
28. Lee, S. Y., Lee, S. Y., Kandala, G., Liou, M.-L., Liou, H. C., and Choi, Y. (1996) CD30/TNF receptor-associated factor interaction: NF-κB activation and binding specificity. *Proc. Natl. Acad. Sci. U.S.A.* **93,** 9699–9703
29. Gotzmann, J., Mikula, M., Eger, A., Schulte-Hermann, R., Foisner, R., Beug, H., and Mikulits, W. (2004) Molecular aspects of epithelial cell plasticity: implications for local tumor invasion and metastasis. *Mutat. Res.* **566,** 9–20
30. Kalluri, R., and Weinberg, R. A. (2009) The basics of epithelial-mesenchymal transition. *J. Clin. Invest.* **119,** 1420–1428
31. Cannito, S., Novo, E., di Bonzo, L. V., Busletta, C., Colombatto, S., and Parola, M. (2010) Epithelial-mesenchymal transition: from molecular mechanisms, redox regulation to implications in human health and disease. *Antioxid. Redox Signal.* **12,** 1383–1430
32. Ryu, H. C., Kim, C., Kim, J. Y., Chung, J. H., and Kim, J. H. (2010) UVB radiation induces apoptosis in keratinocytes by activating a pathway linked to "BLT2-reactive oxygen species." *J. Invest. Dermatol.* **130,** 1095–1106
33. Huber, M. A., Azoitei, N., Baumann, B., Grünert, S., Sommer, A., Pehamberger, H., Kraut, N., Beug, H., and Wirth, T. (2004) NF-κB is essential for epithelial-mesenchymal transition and metastasis in a model of breast cancer progression. *J. Clin. Invest.* **114,** 569–581
34. Richmond, A. (2002) NF-κB, chemokine gene transcription and tumour growth. *Nat Rev. Immunol.* **2,** 664–674
35. Oft, M., Akhurst, R. J., and Balmain, A. (2002) Metastasis is driven by sequential elevation of H-ras and Smad2 levels. *Nat. Cell Biol.* **4,** 487–494
36. Derynck, R., and Zhang, Y. E. (2003) Smad-dependent and Smad-independent pathways in TGF-β family signalling. *Nature* **425,** 577–584
37. Valcourt, U., Kowanetz, M., Niimi, H., Heldin, C. H., and Moustakas, A. (2005) TGF-β and the Smad signaling pathway support transcriptomic reprogramming during epithelial-mesenchymal cell transition. *Mol. Biol. Cell* **16,** 1987–2002
38. Nieto, M. A. (2002) The snail superfamily of zinc-finger transcription factors. *Nat. Rev. Mol. Cell Biol.* **3,** 155–166
39. Barberà, M. J., Puig, I., Domínguez, D., Julien-Grille, S., Guaita-Esteruelas, S., Peiró, S., Baulida, J., Francí, C., Dedhar, S., Larue, L., and García de Herreros, A. (2004) Regulation of snail transcription during epithelial to mesenchymal transition of tumor cells. *Oncogene* **23,** 7345–7354
40. Strippoli, R., Benedicto, I., Pérez Lozano, M. L., Cerezo, A., López-Cabrera, M., and del Pozo, M. A. (2008) Epithelial-to-mesenchymal transition of peritoneal mesothelial cells is regulated by an ERK/NF-κB/Snail1 pathway. *Dis. Model Mech.* **1,** 264–274
41. Chua, H. L., Bhat-Nakshatri, P., Clare, S. E., Morimiya, A., Badve, S., and Nakshatri, H. (2007) NF-κB represses E-cadherin expression and enhances epithelial to mesenchymal transition of mammary epithelial cells: potential involvement of ZEB-1 and ZEB-2. *Oncogene* **26,** 711–724
42. Felton, V. M., Borok, Z., and Willis, B. C. (2009) *N*-Acetylcysteine inhibits alveolar epithelial-mesenchymal transition. *Am. J. Physiol. Lung Cell Mol. Physiol.* **297,** L805–L812
43. Boudreau, H. E., Casterline, B. W., Rada, B., Korzeniowska, A., and Leto, T. L. (2012) Nox4 involvement in TGF-β and SMAD3-driven induction of the epithelial-to-mesenchymal transition and migration of breast epithelial cells. *Free Radic. Biol. Med.* **53,** 1489–1499